A CRYSTAL CHEMICAL INVESTIGATION OF CR SUBSTITUTION IN MUSCOVITE BY XANES SPECTROSCOPY

A. Cardelli[1], G. Cibin[1], M. Benfatto[1], S. Della Longa[2], M.F. Brigatti[3], A. Marcelli[1]

[1]*I.N.F.N., Laboratori Nazionali di Frascati, I-00044 Frascati, Italy*
[2]*Dipartimento Medicina Sperimentale, Universita L'Aquila, via Vetoio –67100 – L' Aquila, Italy, and INFM – Universita' Roma I, P.za A. Moro 1, 00185 – Roma, Italy*
[3]*Dipartimento di Scienze della Terra, Universita'degli Studi di Modena e Reggio Emilia, Largo S. Eufemia 19, I-41100 Modena, Italy*

Abstract

This work introduces a novel procedure to fit the scattering features of XANES spectra. The procedure was applied and validated on a chromium containing muscovite for which structural and crystal chemical characterization is available from literature. The simulation, which involved clusters formed by up to 90 atoms, proved to be effective in representing the Cr local environment, even if the system is characterized by a very low metal content, as demonstrated by the extremely good correspondence with experimental data.

Submitted to Physics and Chemistry of Minerals

1 – INTRODUCTION

Muscovite (ideally, $^{[12]}K\ ^{[6]}Al2\ ^{[4]}(Si_3Al)\ O_{10}\ (OH)_2$), a common rock-forming mineral, can host different cations at tetrahedral and octahedral positions (Brigatti and Guggenheim 2002). Conventional crystallographic methods sometimes proved to be not fully effective in representing the local metal environment in muscovite samples despite its significance as petrogenetic indicator. Information on site occupancy, cation ordering, transition metal oxidation state can thus be difficult to obtain form traditional x-ray diffraction experiments.

Aim of this work is thus to describe Cr local environment (oxidation state, site occupancy and local distortion) in a low Cr-containing system starting from a novel approach involving the simulation of the multiple scattering features of XANES spectra deriving from substitution patterns involving tetrahedral, octahedral and interlayer sites.

2 – EXPERIMENTAL PROCEDURES

2.1 – Sample

Brigatti et al. (2001) performed a crystal chemical study on the Cr-containing muscovite under investigation, starting from different analytical techniques. This sample is from North Westland glacial moraines (New Zealand) and shows the following composition $^{[12]}(K_{0.857}Ba_{0.044}Na_{0.103})\ ^{[6]}(Al_{1.858}Ti_{0.003}Fe^{2+}_{0.039}Cr^{3+}_{0.062}Mg_{0.081})\ ^{[4]}(Si_{3.110}Al_{0.89})\ O_{10.166}\ (OH)_{1.829}$ $Cl_{0.005}$, thus being characterized by moderate homovalent and heterovalent substitutions that involve octahedral, tetrahedral and interlayer positions. Single crystal structure refinements give tetrahedral mean bond distances (<T-O>= 1.646(1) Å for both T1 and T2 tetrahedra) very close to the end member muscovite (<T1-O> = 1.646(5) Å and <T2-O> = 1.647(5) Å) (Guggenheim et al. 1987). The mean electron counts for the cis-octahedral site (M2), greater than 13, pointed out that cations heavier than Al were located at the M2 site. Furthermore, the <M2-O> mean bond distance is very close to muscovite (<M2-O> = 1.931(1) Å in sample from Westland; <M2-O> = 1.935(5) Å in muscovite, Guggenheim et al. 1987). Unlike muscovite, where the trans-octahedral cavity (M1) is completely empty, this sample showed residual areas of positive electron densities in the M1 position, suggesting a M1 partial occupancy. These results suggested a Cr preference for the octahedral sites, but could not return definite evidence about Cr ordering at the two independent octahedral sites and about the local structural arrangement that the metal imparts to the layer.

2.2 – XANES spectra

XANES spectra of chromium-containing muscovite were obtained at the GILDA (BM8) beamline, European Synchrotron Radiation Facility. Muscovite powder samples were prepared by fine grinding and deposition on a millipore membrane. Experiments were performed, using a double crystal monochromator equipped with Si(311) crystals, at 0.5 eV resolution in fluorescence mode using a 13 elements Ge detector. Typical acquisition time was 3s, and energy calibration was

carried out using a reference Cr foil. The experimental data spectra were background subtracted, normalized at high energy using a standard procedure and averaged. Due to the low concentration, the signal/noise ratio obtained at the Cr K edge is about 10^3.

2.3 – Theoretical method

The XANES analysis was carried out by using a new program, MXAN, which is able to perform a quantitative analysis of the spectra (Benfatto and Della Longa 2001, Della Longa et al. 2001). This method is based on the comparison between the experimental data and several simulations performed by varying selected structural parameters starting from a given geometrical configuration around the absorber atom. The photoabsorption cross-section is calculated using the full multiple scattering (MS) scheme in the framework of the muffin-tin approximation for the shape of the potential. Muffin-tin radii are calculated on the basis of the Norman criterion with a 2 % of overlapping. Details of the method can be found in (Tyson et al. 1992, Hedin and Lundqvist 1969, Gelatt et al. 1983, Benfatto and Della Longa 2001 and Della Longa et al. 2001). In this work the best fit calculations are made by using a cluster of 89 atoms.

3 – RESULTS AND DISCUSSION

The bottom curve in Fig.1 reports the Cr K edge absorption spectrum obtained on the chromium-containing muscovite from Westland. The spectrum is similar to the ones reported by Brigatti et al. (2001), obtained on Cr-bearing muscovite samples, and exhibits a higher signal to noise ratio. This resolution allows the identification of a clear double pre-edge structure (Fig. 1, inset) with relative maximum values at 5998.5 and 5990.5 eV. Two contributions (A and A') can be observed at the rising edge. They are followed by a double main structure (peaks B and C) with two maximum values at 6008.5 and 6020.2 eV, respectively. The spectrum is characterized by broad features in the intermediate multiple scattering (IMS) region and almost three contributions can be here identified: D, E and F. Two minor features (G and H) follow at around 6105 and 6135 eV and precede the first main EXAFS oscillation (I) at 6168 eV.

XANES data and particularly the presence of a pre-edge structure, following a transitions to d empty states in a distorted octahedral entity, support the octahedral coordination of Cr. A previous estimation (Brigatti et al. 2001) determined an upper limit for the presence of Cr in tetrahedral coordination to less than 0.5% of the total chromium content. This value was obtained from a fit procedure of the pre-edge with gaussian components and from the comparison with the tetrahedrally coordinated model compound $SrCrO_4$.

Given the Cr octahedral coordination, a further development involves the identification of the octahedral site at which Cr is preferentially located. An attempt is here made to distinguish between the two possible octahedral sites that could host Cr in muscovite.

The trans-octahedral (M1) and the cis-octahedral (M2) sites, as determined by XRD, are different in topology. In particular their different mean bond lengths, <M1-O> and <M2-O>, reflect different electrostatic interactions on neighbouring oxygen atoms (<M2-O> = 1.931(1) Å; <M1-O> = 2.244(1) Å). M2 site is not only smaller, but also less distorted than M1 site (octahedral angle variance, OAV = 109.2$^{\circ 2}$ and 58.7$^{\circ 2}$ for M1 and M2 site, respectively). Furthermore in the 2:1 layer of dioctahedral micas (space group C2/c), each cis-octahedral site (M2) is surrounded by three other equivalent cis-octahedra and by three empty M1 cavities, whereas the trans-octahedral cavity is confined by six cis-octahedra, thus accounting for a different topology and different interactions both inside and outside the octahedral sheet (Ferraris and Ivaldi 2002). Following these structural
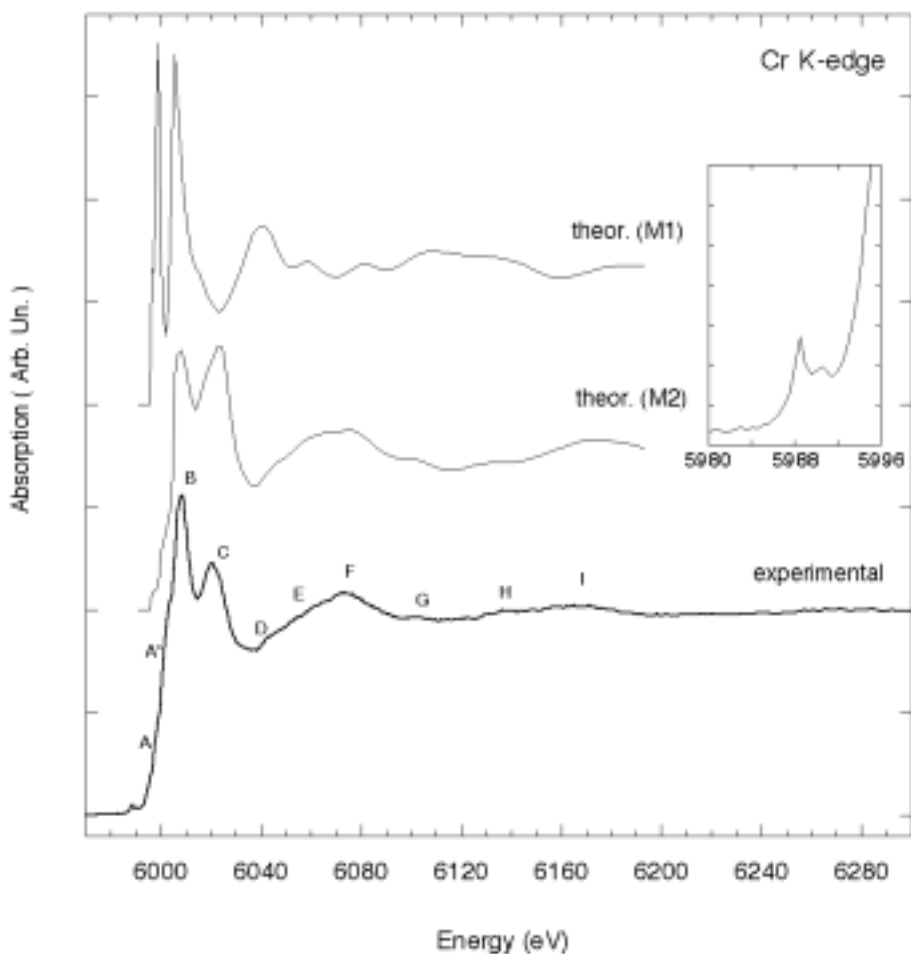

FIG.1 Comparison between the experimental (bottom) Cr K-edge absorption spectrum of chromium-containing muscovite from Westland (NZ) and the theoretical results of the two octahedral clusters: M1 (top) and M2 (middle). The inset enlarge the pre-edge region of the experimental spectrum. The energy values refer to the experimental data.

considerations, the Cr K-edge absorption simulated spectra are significantly different if chromium is set at M1 or at M2 position. Fig. 1 reports the comparison between the simulated spectra assuming for Cr a M1 (top spectra) or M2 (middle spectra) occupancy. More consistent results with experimental data were obtained under the hypothesis of M2 occupancy, whereas when Cr is placed at M1, simulated spectra and experimental data mostly differs in the distance between the two main features (about 7 eV for M1) and for the presence of a sharp contribution ~40 eV above the absorption edge. In this way both the octahedral coordination for Cr is confirmed, as supported by the pre-edge analysis also, and the relative occupancy of Cr at M1 site is below the detection limit in Westland muscovite.

Fig. 2 reports the effect of an increase of the number of atoms around the absorber on the evolution of the Cr spectral features. An 89 atoms cluster, corresponding to a distance of 6.4 Å far
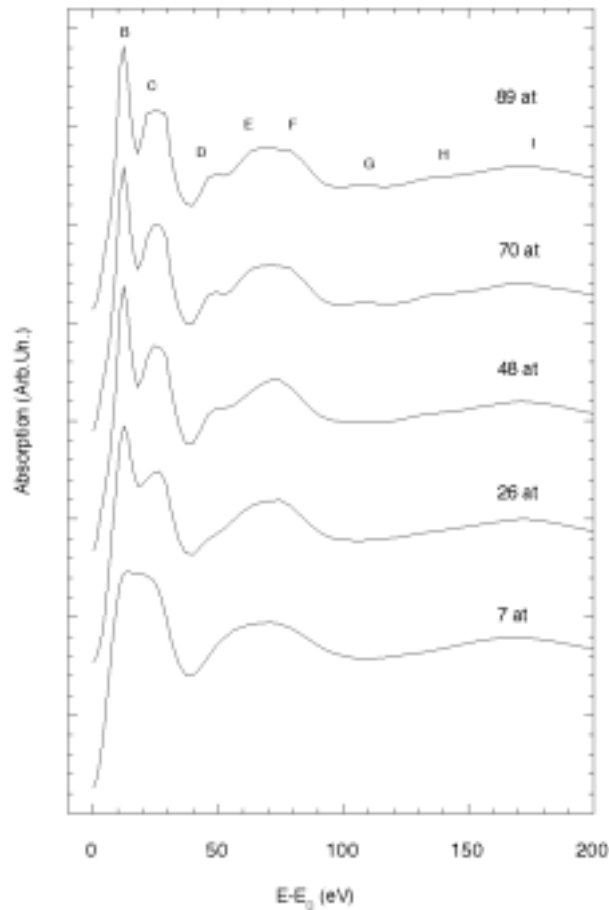

FIG. 2. Theoretical spectra at the Cr K edge for an octahedral M2 surrounding cluster of increasing size from 7 up to 89 atoms. The energy values referre to the threshold energy E_0.

from the absorber, can be considered as optimal, following the convergence of the total cross section with respect to the number of atoms. No significant difference in simulated spectra was in fact observed moving from 70 to 89 atoms in the cluster. Features E and F are only present in clusters including the potassium cations nearest to the photoabsorber. The interlayer cation is thus the nearest neighbour of the octahedron and it is placed in the tetrahedral cavity at a distance of approximately 5.3 Å from the centre of M2. More quantitative structural information on the Cr local environment can be obtained from the MXAN package, considering only some possible structural deformations induced by Cr over an unperturbed lattice. Fig. 3 presents the effects of some structural variations around Cr.

A set of MS simulations was thus performed assuming different displacement modes of the atomic groups in different planes and along different directions. The intensity and energy variations of the spectral features were considered as indicators of the agreement with experimental data and of the most sensitive structural parameters.

A rigid displacement of the upper and lower octahedral surfaces characterizes the first set of spectra (referred as [1]). Each octahedral surface is formed by groups of three oxygen atoms along [001] direction. The induced Cr-O distance variations are correlated to the main oscillation maximum and the relative intensity of the D-E-F features slightly modify together with the B/C height ratio. The second set (referred as [2]) relates to the effect of the simultaneous radial displacement in the (001) plane of three atom groups, each composed by two near octahedral O vertex rigidly linked to the Al atom nearest to Cr in the M2 position. Each of these groups is moved in the Cr-Al bond direction. Like the first set, the second set of spectra is characterized by the shift of the I feature, due to the Cr-O distance variation, and by the modification of the weight of the G and H structures. The F peak becomes more evident when the Cr-Al distance increases. The intensity and the position of the main B and C peaks are strongly influenced by these distortions. The last set of spectra (referred as [3]) is associated to the movement of the nearest tetrahedra.

The basal oxygen atom of the four tetrahedra nearest to M2, two below and two above the octahedral sheet, were connected to the Si atoms placed at their centre, thus forming two atomic groups opposite with respect to the octahedral sheet. Those groups were moved in the direction defined by the adsorber and by the oxygen atoms shared between the tetrahedra.

This displacement induces only minor spectral changes, mostly involving G and H features that become more separated and strong with an increase of the Cr-T distance. However the entire IMS region is weakly affected by this latter distortion. Other structural modifications, like the substitution of Si for Al in the T sites, induces even smaller effects on the spectral features.

The calculation so far presented thus allowed the identification of the parameters to be used in the final fitting procedure of the experimental data. A first fit of the experimental spectrum was performed moving the upper and lower octahedral surfaces in the [001] direction, as described in [1]. This movement is independent from [2] and [3], because
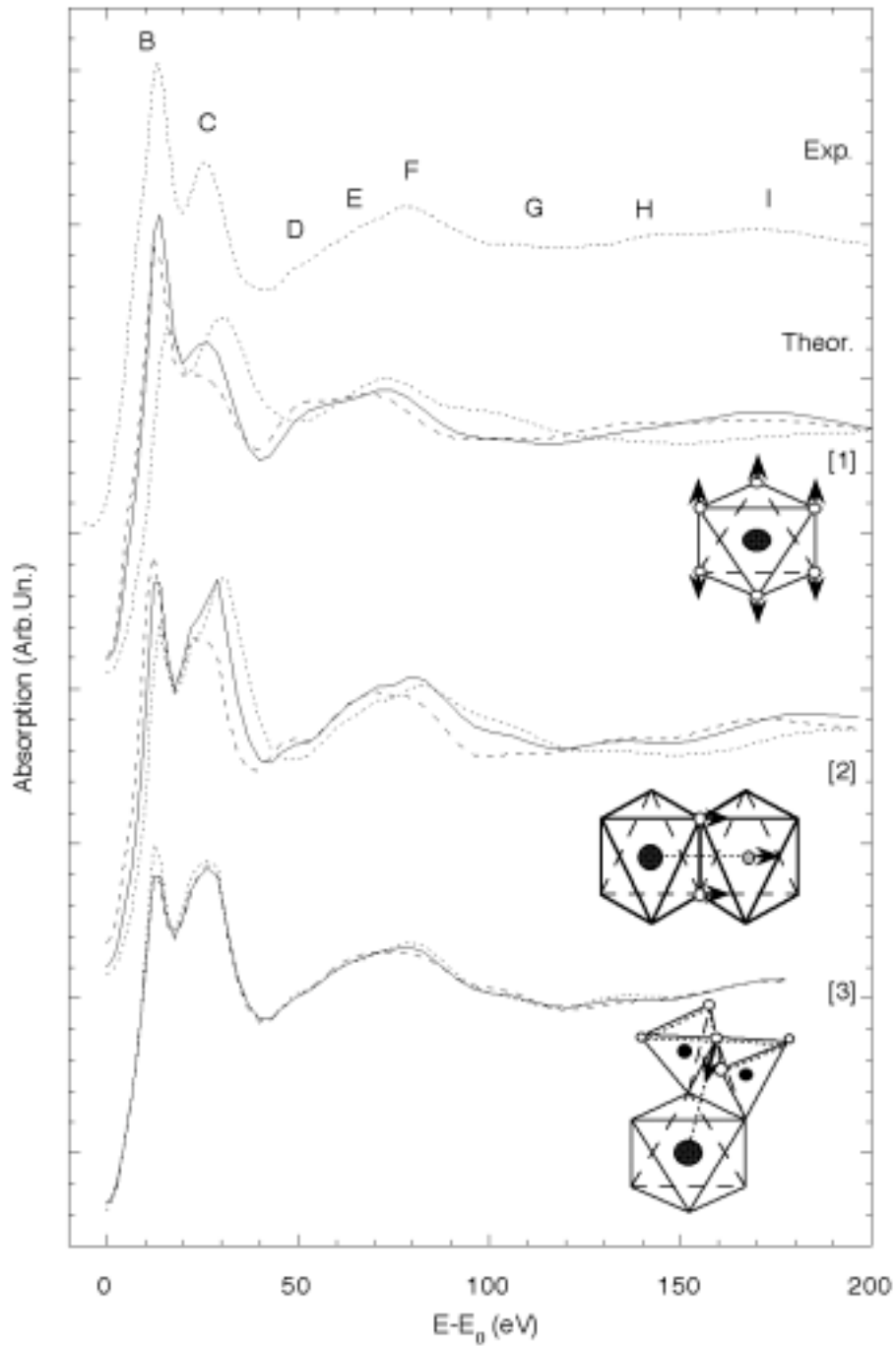
FIG. 3. Effect of several displacement modes of the entities surrounding Cr at M2 site over simulated Cr K-edge spectra. The top curve reports the experimental spectrum. The tree other are the simulated spectra referring to displacement modes [1], [2], and [3], as defined in the text. Schematic drawings of the cluster deformation are included. The energy scale is the same of Fig.2.

MXAN program only allows for separate fitting simulations when atomic displacements are described in cartesian or polar coordinates.

The minimization procedure converged on a vertical displacement of 0.10±0.01 Å. A new initial configuration was thus derived from this best fit result and the process was iterated for the two remaining radial movements ([2] and [3]). A MINUIT fit convergence showing an almost diagonal (2 ´ 2) correlation matrix between the parameters was obtained. The final fit result is reported in Fig. 4 and compared with the reference experimental spectrum. In the lower part of Fig. 4, the absorption spectrum calculated using the initial atomic configuration resulting from the diffraction data is reported for comparison. The agreement between the experimental data and the result of the fitting procedure is very good, both in intensity and position of all the spectral features, confirming the occupancy of Cr at M2. Furthermore, the atomic positions resulting from the fitting procedure show a slight enlargement of the octahedron (ΔR=+0.011±0.001 Å) in (001) and a reduction of the radial distance of the near tetrahedra (ΔR= -0.05±0.02 Å). The final radial displacement of the first oxygen shell and of the second shell tetrahedra is reported in Table 1.

TABLE 1. Comparison between M2 site bond lengths obtained by X-ray diffraction analysis and XANES fitting results. <Cr-O(tetr)> indicates the distance between Cr and oxygen atoms shared between two nearest tetrahedra considered in the calculation (see fig. 4 for detail).

	XRD	fit result	variation
Cr-O31	1.948(1)	2.01(1)	0.06(1)
Cr-O31'	1.924(1)	1.99(1)	0.06(1)
Cr-O32	1.925(1)	1.98(1)	0.06(1)
Cr-O32'	1.946(1)	2.02(1)	0.07(1)
Cr-O4	1.919(1)	1.99(1)	0.07(1)
Cr-O4'	1.921(1)	1.98(1)	0.06(1)
<Cr-Al>	3.000(1)	3.013(1)	0.012(1)
<Cr-O (tetr.)>	3.411(1)	3.36(2)	-0.05(2)

The relative variation of the distances from the absorber are +3.4% and -2.1%, respectively. The displacement of Al atoms in (001) is +1.2% .The octahedron enlargement is particularly significant when compared to the diffraction data obtained in a Cr-rich mica (Evsyunin et al., 1997), where Cr substitutes for up the 80% of Al in the octahedra. The Cr octahedral average size obtained in the simulation process (1.99±0.01 Å) matches very well the <M2-O> value reported for this Cr-rich mica (1.976(3) Å). The non-structural parameters fitted in the final atomic configuration are all consistent. The Gc value (2.03 eV) representing the energy independent spectral broadening is in agreement with the core-hole lifetime broadening value, i.e. the natural

width of the Cr K atomic level (1.08 eV) (Krause and Oliver 1979) , which needs to be combined with the experimental energy resolution. The fitted inelastic losses broadening presents energy threshold and amplitude (respectively 16.58 eV and 6.66eV), corresponding to the right plasmon excitation energy and amplitude (Benfatto and Della Longa 2001, Tyson et al. 1992).
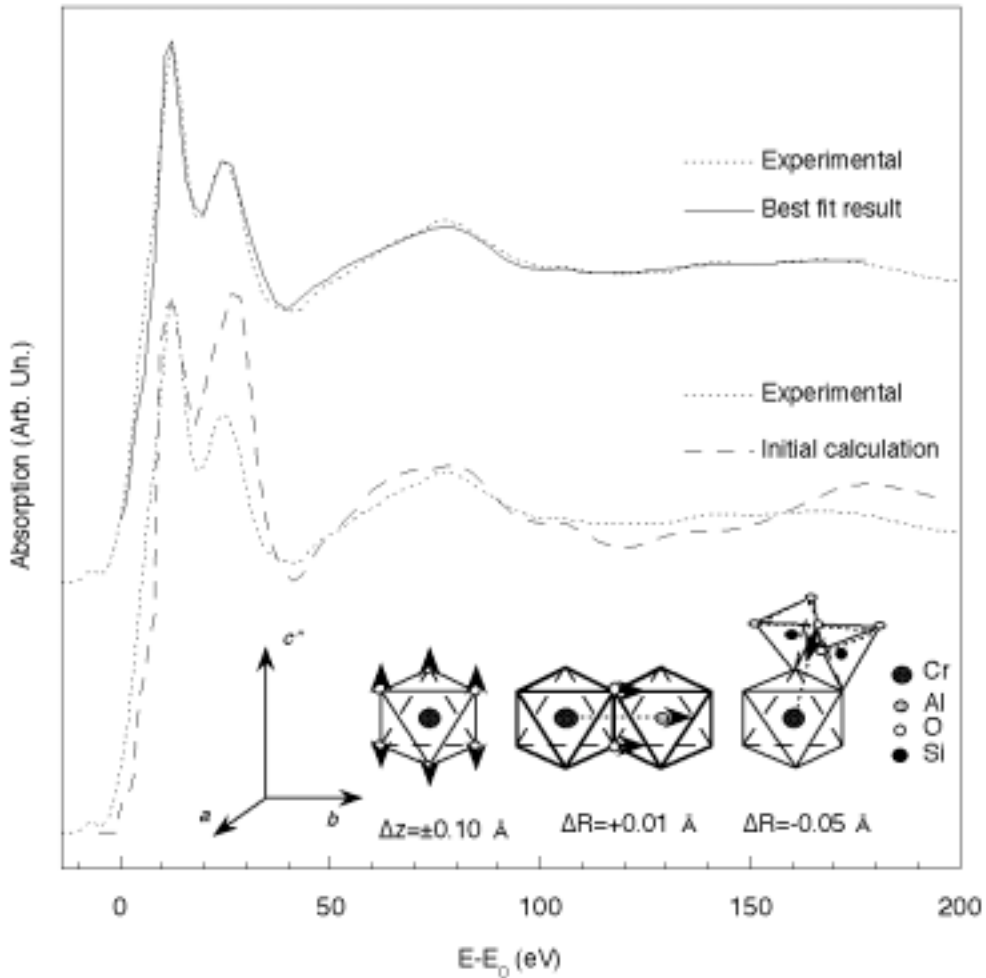

FIG. 4. Comparison between experimental data and the best fit from MXAN procedure. The schematic drawing of the displacement of entities surrounding Cr, which is introduced in the fitting procedure, is included with the distortion parameters obtained as a final result. The energy scale is the same of Fig.2.

4 – CONCLUSIONS

Diffraction techniques are powerful method to characterize natural crystalline systems and in particular to determine mean bond distances. However, the local distortions are very difficult to be investigated and this task becomes very difficult when the concentration of the atom under investigation is low. The X-ray absorption spectroscopy, on the contrary, is sensitive to the local environment and it is recognised as a specific method to characterize local coordination and geometrical arrangements i.e., bond distances and bond angles (Mottana et al. 2002). The improvements achieved in the fitting procedure of the XANES spectra are clearly demonstrated in this manuscript, where the local geometry was correctly described even in the case of very low substitution and additional potential capabilities never applied before with this spectroscopy are opened for the study of minerals.

The simulation reported in this manuscript demonstrate that it is possible to improve both in term of local geometrical description and quantitative determination of the distances any previous calculations. The analysis performed on the spectra of Cr-muscovite under investigation confirms the previous assignment (Brigatti et al. 2001) concerning the octahedral occupancy, but reduces significantly the value of the upper limit occupancy of one of the two possible octahedral site (M1) versus the other (M2). The accuracy of the simulation is excellent and the different possible distortions of the structure were modelled and discussed. In particular, the best fit is obtained when the contribution of the interlayer cation, a basic ingredient of the mica structure is included and distortions of the octahedra are taken into account. In this case distortions induced by atomic displacements far over the second shell were demonstrated to be substantially negligible.

5 – ACKNOWLEDGEMENTS

REFERENCES

(1) M. Benfatto, S. Della Longa: J. Synchr.Rad. 8, 1087-1094 (2001)

(2) M.F. Brigatti, S. Guggenheim Mica crystal chemistry and the influence of pressure, temperature, and solid solution on atomistic models. In: Micas: crystal chemistry and metamorphic petrology. Ed. A. Mottana, F.P. Sassi, J.B. Thompson, Jr. and S. Guggenheim, Review in Mineralogy & Geochemistry 46, 1-97 (2002).

(3) M.F. Brigatti, E. Galli , L. Medici , L. Poppi , G. Cibin , A. Marcelli and A. Mottana: Eur. J. Mineral 13, 377-389 (2001).

(4) S. Della Longa, A. Arcovito, M. Girasole, J.L. Hazemann, M. Benfatto: Phys. Rev. Lett. 87, 155501-155504 (2001).

(5) V. G. Evsyunin, A. A. Kashaev and R. K. Rastsvetaeva: Crystallography Reports 42, 571-574 (1997).

(6) G. Ferraris, G. Ivaldi Structural features of micas. In: Micas: crystal chemistry and metamorphic petrology. Ed. A. Mottana, FP Sassi, JB. Thompson, Jr., S Guggenheim. Review in Mineralogy & Geochemistry 46, 117-153 (2002).

(7) S. Guggenheim, Y.-H. Chang, and A. F. Koster van Groos: Am. Mineral. 72, 537-550 (1987).

(8) C.D. Gelatt, S. Kirkpatrick, M.P. Vecchi: Science 220, 671-681 (1983).

(9) L. Hedin, S. Lundqvist Effects of Electron-Electron and Electron-Phonon Interactions on the One-Electron States of Solids. In: Solid State Physics. Ed. F. Seitz F, D. Turnbull, H. Ehrenreich (Academic Press, New York 1969) vol. 23, pp. 1-15.

(10) M. O. Krause, J. H. Oliver: Phys. Chem. Ref. Data 8, 329 (1979).

(11) A. Mottana, A. Marcelli, G. Cibin, M.D. Dyar X-ray absorption spectroscopy of the micas. In: Micas: crystal chemistry and metamorphic petrology. Ed. A. Mottana, FP Sassi, JB. Thompson, Jr., S Guggenheim. Review in Mineralogy & Geochemistry 46: 371-411. (2002).

(12) T. A. Tyson, K. O. Hodgson, C.R. Natoli, M. Benfatto: Phys. Rev. B 46, 5997-6019 (1992).